Central European Journal of Energetic Materials
ISSN 1733-7178; e-ISSN 2353-1843

Cent. Eur. J. Energ. Mater. 2018, *15*(2): 225-242; DOI: 10.22211/cejem/92221

Investigation of the Radical Nitration of Isooctane Fuel *via* Nitromethane Propellant

Caglar Celik Bayar

Department of Metallurgical and Materials Engineering, Bulent Ecevit University, 67100 Zonguldak, Turkey
E-mail: caglarbayar@gmail.com; *caglarbayar@beun.edu.tr*

Abstract: The possible radical nitration reactions of isooctane fuel with nitromethane propellant, which is generally used as an additive in fuel formulations, were thermodynamically investigated both at room temperature and at a higher temperature of 691.15 K. The temperature of 691.15 K was chosen because it is the auto-ignition temperature of isooctane and nitromethane and has the potential to mimic better engine conditions. The computational calculations were performed at the theoretical level of DFT UB3LYP/cc-pVDZ. Four different nitration reactions and nitrated products were considered and interpreted in detail. The most and the least favorable nitrations were observed at the primary and secondary carbons of isooctane at 691.15 K, respectively. Four of the designated reactions were endothermic at this temperature. The other outcome of this study was that there was a direct relationship between the thermodynamic tendencies of the considered reactions and the ballistic performances (detonation velocities, detonation pressures, and specific impulses) of their nitrated products. The thermodynamic properties of heats of combustion and deflagration temperatures were calculated *via* empirical formulations based on the stoichiometry and some other structural parameters of the energetic materials. The results for nitromethane and the nitro-isooctane products were examined.

Keywords: nitromethane, isooctane, nitration, specific impulse, Dunning basis sets

1 Introduction

Isooctane (2,2,4-trimethylpentane) is a clear colorless liquid [1] with a petroleum-like odour [2]. It is less dense than water (0.6919 g/cm^3) [2] and

its flash point is low (4.5 °C) [3]. It is used as one of the model fuel species in both modelling and experimental studies on spark and homogeneous charge compression ignition engines. It is used both as a neat fuel and as a major component in a primary reference fuel blend. Isooctane also serves to define the 100 point on the octane rating scale and is a primary reference fuel for octane rating in spark-ignition engines [4].

Another component in the present study is nitromethane, which is a clear, colorless liquid at room temperature. It possesses very low toxicity, is relatively inexpensive and easily obtainable compared to the well-known and widely used monopropellant hydrazine. It can be stored and handled safely under normal laboratory conditions. Another advantage of nitromethane is it has a higher density (ρ) and specific impulse (I_{sp}) than hydrazine ($\rho_{(Nitromethane)} = 1.127$ g/cm^3, $\rho_{(Hydrazine)} = 1.013$ g/cm^3; $I_{sp(Nitromethane)} = 276$ s, $I_{sp(Hydrazine)} = 234$ s). The energy density of nitromethane coupled with its good thermal stability and low toxicity make it ideal for the laboratory testing of small-scale propulsion devices. It is used in a variety of combustion applications, as a monopropellant, as a fuel admixed with methanol for "Top Fuel" drag racing and as an additive to other fuels to improve performance in small combustion chambers [5].

Nitro-alkanes are known as fuel components. They increase the available specific energy of a combustible air/fuel mixture in an engine [6-10]. However they are not available for use as a fuel in their pure form because of their shock sensitivity; they can be used as a blending component within a fuel formulation [9, 10]. Nitromethane, one of these nitro-alkanes, is used within formulations containing high amounts of isooctane. Simple bond rupture of nitromethane in an engine was suggested as producing methyl and nitro radicals as shown below [10].

$$CH_3NO_2 \rightarrow CH_3. + NO_2. \quad (1)$$

The present computational study covers the investigation of the radical nitration of isooctane fuel *via* nitromethane propellant, which is usually used as an additive material to increase the engine power. The reaction sequence considered was as follows: The first step was the investigation of the possible homolytic bond dissociation reactions of isooctane fuel. In these reactions, primary, secondary and tertiary radicals of isooctane are generated together with hydrogen radicals. In the second step, the homolytic bond dissociation reaction of nitromethane occurs as presented in the reaction above. In the third step, the reactions of the generated isooctane radicals with nitro radicals are investigated. The last step includes the formation of methane *via* the combination of methyl and hydrogen radicals.

The Gibbs free energies for all of the reaction steps were calculated to estimate the most spontaneous reaction at 1 atm. The Kamlet-Jacobs detonation performances (detonation velocity and detonation pressure) of nitromethane and of all nitro-isooctane species were calculated using the computed crystal densities. Finally, the computed crystal densities and detonation velocities were used to obtain and compare the specific impulse values of nitromethane and nitro-isooctane derivatives in their crystalline forms. Since such a study and its pathways have not been investigated before, they appear as an original work.

2 Methods of Calculation

The initial structure optimizations leading to the energy minima were performed using the MM2 method followed by the semi-empirical PM3 self-consistent field molecular orbital (SCF-MO) method [11] and Hartree-Fock (HF) SCF-MO methods [12] at the unrestricted level. Further optimizations were performed within the framework of Density Functional Theory (DFT), with the B3LYP functional [13] at the unrestricted level of a cc-pVDZ basis set. The exchange term of B3LYP consists of hybrid Hartree-Fock and local spin density (LSD) exchange functions with Becke's gradient correlation [14]. The correlation part of B3LYP consists of the VWN3 local correlation functional by Vosko, Wilk and Nusair [15] and the LYP correlation correction functional by Lee, Yang and Parr [16].

All vibrational analyses and thermochemical calculations were performed using DFT UB3LYP/cc-pVDZ level of theory. The vibrational analyses had no imaginary frequencies, which indicated that no transition states or saddle points were observed on the potential energy surfaces. The Gibbs free energy changes were calculated both at 298.15 K and 691.15 K, the latter being the auto-ignition temperature of isooctane and nitromethane [3, 17], at 1 atm. The Gibbs free energy changes of the radical reactions were corrected with basis set superposition error (BSSE) contributions [18, 19]. BSSE corrections use the Boys and Bernardi counterpoise technique [18, 20], which are due to overlap of the wave functions of the moieties [21]. The ballistic performances of nitromethane and nitro-isooctane derivatives in their crystalline states were calculated using the formula presented by Kamlet and Jacobs [22]. The specific impulse values of solid nitromethane and nitrated isooctane products were calculated according to Keshavarz's empirical equation [23, 24]. All of the computations were performed for the gas phase using the Gaussian 09 software package [25].

3 Results and Discussion

3.1 Basis set selection

The basis set selection in this study depended on a good prediction of the computationally derived crystal density of nitromethane. Solid nitromethane has $P2_12_12_1$ space group and lattice vectors of a = 5.183 Å, b = 6.236 Å and c = 8.518 Å [26]. It contains 28 atoms (4 molecules) in its unit cell, with a unit cell volume of 275.31 Å^3 [26-28]. The crystal density of nitromethane does not, to the best of knowledge, appear in the literature but it can be calculated in the light of the number of molecules per unit cell and unit cell volume information. Consequently, it was found to be 1.47 g/cm^3. In the study, the molar volumes of nitromethane were computed with 12 different Pople and Dunning basis sets in order to find the best crystal density. It should be noted that the molar volume calculations use Monte Carlo integration technique implemented in the Gaussian 09 software package, with the space enclosed by the 0.001 au (electrons/bohr^3) contour of the molecule's electron density, as proposed by Bader *et al*. [29]. The crystal densities were then calculated by division of the molecular weight of nitromethane by its computed molar volumes (obtained with different basis sets). The closest density value belonged to the DFT UB3LYP/cc-pVDZ level of calculation, 1.48 g/cm^3 (Table 1).

Table 1. Computed molar volumes and calculated crystal densities of nitromethane with different Pople and Dunning basis sets of DFT UB3LYP theoretical level

Method: DFT , Functional: UB3LYP		
Basis set	V [cm^3/mol]	ρ [g/cm^3]
6-31G(d,p)	42.78	1.43
6-31+G(d,p)	43.97	1.39
6-31++G(d,p)	43.35	1.41
6-311G(d,p)	43.58	1.40
6-311+G(d,p)	43.31	1.41
6-311++G(d,p)	43.09	1.42
cc-pVDZ	41.16	1.48 (1.47)[a)]
aug-cc-pVDZ	43.80	1.39
cc-pVTZ	43.70	1.40
aug-cc-pVTZ	43.86	1.39
cc-pVQZ	44.88	1.36
aug-cc-pVQZ	43.21	1.41

[a)]Data in parenthesis is the experimental crystal density of nitromethane calculated in the light of the unit cell information obtained from Refs. [26-28].

Figure 1 shows the atom numberings of nitromethane. Table 2 lists the computed structural parameters of nitromethane (bond lengths and bond angles) with the basis sets used in Table 1. However, almost all of the basis sets produced structural parameters closer to the experimental ones [30]; the cc-pVDZ basis set was an advantageous one overall in terms of computing a better crystal density at the same time (Tables 1 and 2). Therefore, it was chosen as an ideal basis set and used in the entire study.

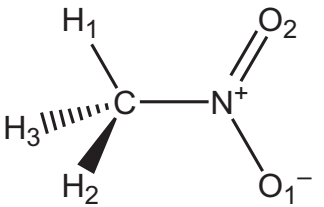

Figure 1. The atom numberings of nitromethane

Table 2. Experimental and computed structural parameters of nitromethane obtained with different Pople and Dunning basis sets at the theoretical level of DFT UB3LYP

Method: DFT , Functional: UB3LYP							
	Exp[a)]	6-31G(d,p)	6-31+G(d,p)	6-31++G(d,p)	6-311G(d,p)	6-311+G(d,p)	6-311++G(d,p)
Bond lengths [Å]							
C−N	1.49	1.50	1.50	1.50	1.50	1.50	1.50
C−H(1)	1.09	1.09	1.09	1.09	1.09	1.09	1.09
C−H(2)	1.09	1.09	1.09	1.09	1.09	1.09	1.09
C−H(3)	1.09	1.09	1.09	1.09	1.09	1.09	1.09
N−O(1)	1.22	1.23	1.23	1.23	1.22	1.22	1.22
N−O(2)	1.22	1.23	1.23	1.23	1.22	1.22	1.22
Bond angles [°]							
NCH(1)	107.5	108.0	108.0	108.0	108.0	108.0	108.0
NCH(2)	107.5	108.0	108.0	108.0	108.0	108.0	108.0
NCH(3)	107.5	106.8	106.6	106.6	106.7	106.5	106.5
CNO(1)	117.4	117.0	117.2	117.2	117.0	117.2	117.2
CNO(2)	117.4	117.0	117.2	117.2	117.0	117.2	117.2
O(1)NO(2)	125.3	126.0	125.5	125.5	126.0	125.6	125.6

Table 2. Cont'd.

Method: DFT , Functional: UB3LYP							
	Exp[a)]	cc-pVDZ	aug-cc-pVDZ	cc-pVTZ	aug-cc-pVTZ	cc-pVQZ	aug-cc-pVQZ
Bond lengths [Å]							
C−N	1.49	1.50	1.50	1.50	1.50	1.50	1.50
C−H(1)	1.09	1.09	1.09	1.08	1.08	1.08	1.08
C−H(2)	1.09	1.10	1.09	1.09	1.09	1.09	1.09
C−H(3)	1.09	1.10	1.09	1.09	1.09	1.09	1.09
N−O(1)	1.22	1.22	1.23	1.22	1.22	1.22	1.22
N−O(2)	1.22	1.22	1.22	1.22	1.22	1.22	1.22
Bond angles [°]							
NCH(1)	107.5	108.6	108.2	108.5	108.4	108.5	108.5
NCH(2)	107.5	107.1	107.0	107.1	107.1	107.1	107.1
NCH(3)	107.5	107.2	107.1	107.2	107.2	107.2	107.2
CNO(1)	117.4	116.3	116.7	116.5	116.6	116.6	116.6
CNO(2)	117.4	117.6	117.8	117.6	117.7	117.7	117.7
O(1)NO(2)	125.3	126.1	125.5	125.8	125.6	125.7	125.6

[a)]The experimental structural parameters were taken from Ref. [30].

3.2 The Gibbs free energies

The possible radical nitration reactions of isooctane with nitromethane were considered both in general and as detailed reaction pathways (Figures 2 and 3). In the general reactions, isooctane and nitromethane combined to produce four different nitro-isooctane products, nitroisooctane 1 to 4 and methane (Figure 2). The interpretation of the detailed reaction pathways in Figure 3 was as follows: The first step of the reactions involved the homolytic bond dissociation of isooctane. The reactions I-A and I-D produced primary isooctane radicals while reactions I-B and I-C produced secondary and tertiary radicals, respectively. Hydrogen radical formation accompanied the formation of all isooctane radicals. In the second step, the homolytic bond dissociation reaction of nitromethane occurred. In the third step, the isooctane radicals combined with nitro radicals. In this step, the products of reactions III-A and III-D were primary nitro-isooctane derivatives, while reactions III-B and III-C gave secondary and tertiary derivatives, respectively. The final step involved the formation of methane *via* combination of methyl and hydrogen radicals.

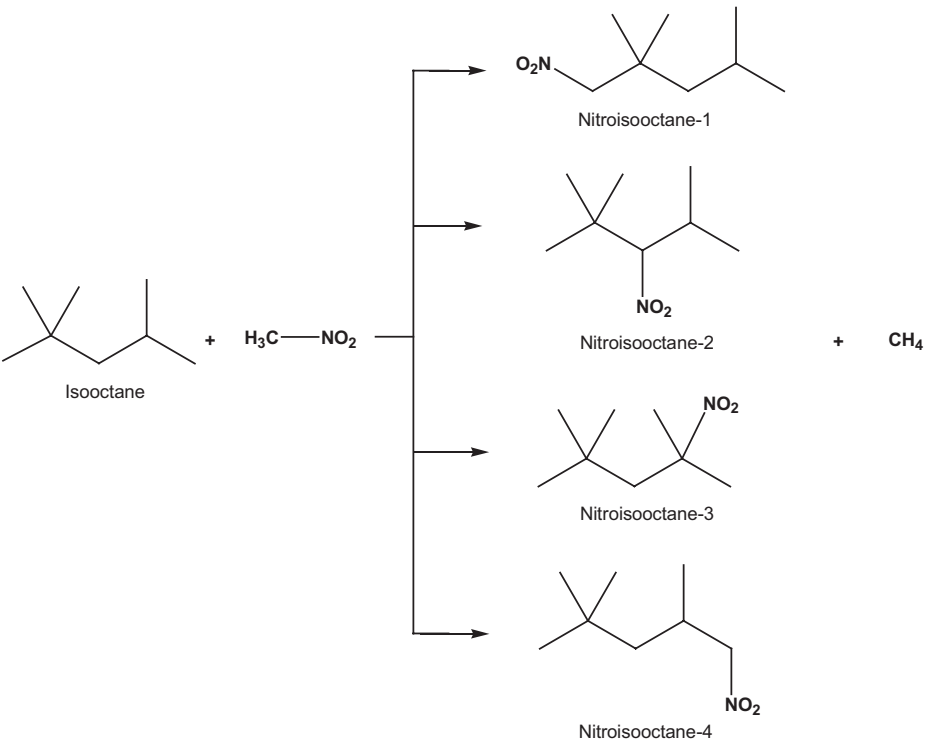

Figure 2. The overall considered radical nitration reactions of isooctane with nitromethane

Accordingly, Table 3 lists the changes in Gibbs free energy (ΔG) of each of these reactions. They were calculated at 1 atm pressure at two different temperatures, 298.15 K and 691.15 K, respectively (691.15 K is the auto-ignition temperature of nitromethane and isooctane [3, 17]). They were calculated separately with and without BSSE corrections [31].

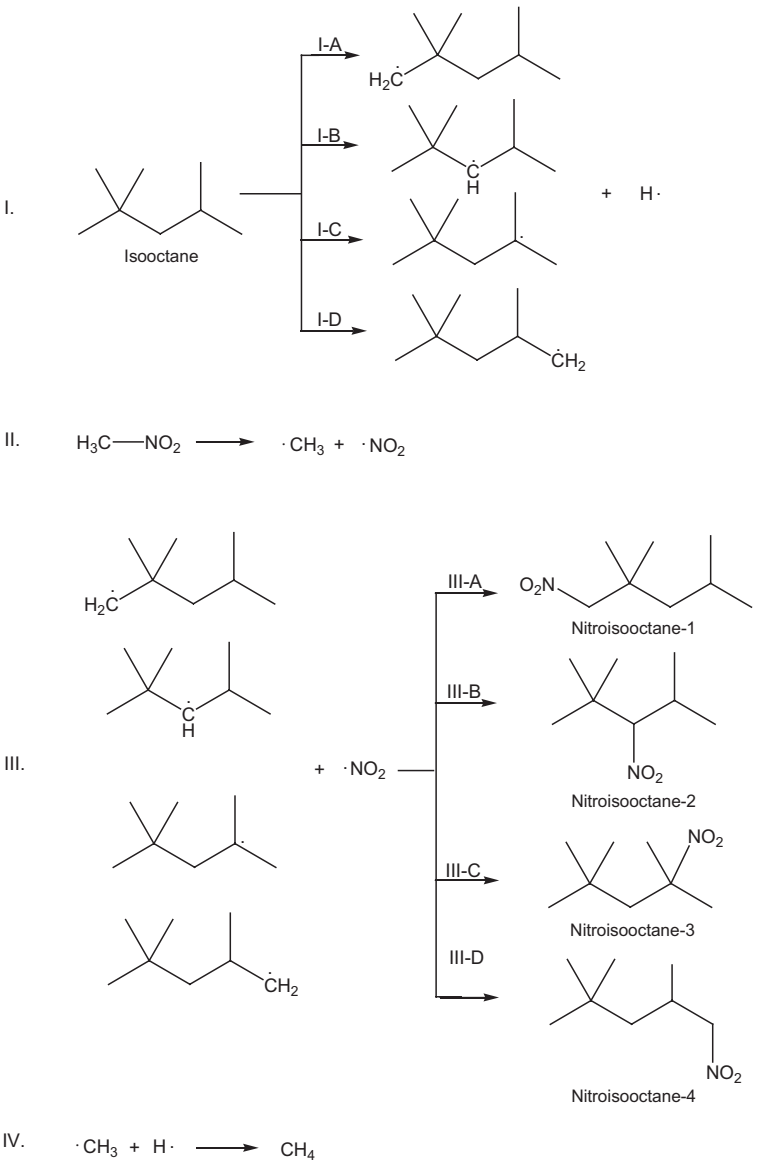

Figure 3. The step by step representation of the considered radical nitration reactions of isooctane with nitromethane

Table 3. Calculated Gibbs free energies of reactions of I-IV at DFT UB3LYP/cc-pVDZ theoretical level

	Gibbs free energy[a)]			
	$\Delta G_{298.15}$	$\Delta G^{B}_{298.15}$	$\Delta G_{691.15}$	$\Delta G^{B}_{691.15}$
Reaction I-A	404.6	402.1	398.6	396.1
Reaction I-B	373.9	371.0	363.3	360.4
Reaction I-C	359.3	356.4	350.1	347.2
Reaction I-D	397.1	394.5	391.7	389.2
Reaction II	179.7	166.5	119.3	106.0
Reaction III-A	−172.1	−150.6	−96.6	−75.1
Reaction III-B	−139.7	−112.5	−54.1	−27.0
Reaction III-C	−135.5	−109.9	−50.9	−25.3
Reaction III-D	−171.5	−151.3	−97.6	−77.4
Reaction IV	−416.3	−414.4	−406.5	−404.6
(I-A + II + III-A + IV) (Formation of Nitroisooctane-1)	−4.1	3.6	14.8	22.4
(I-B + II + III-B + IV) (Formation of Nitroisooctane-2)	−2.4	10.6	22.0	34.8
(I-C + II + III-C + IV) (Formation of Nitroisooctane-3)	−12.8	−1.4	12.0	23.3
(I-D + II + III-D + IV) (Formation of Nitroisooctane-4)	−11.0	−4.7	6.9	13.2

[a)]Energies are in kJ/mol. The BSSE-corrected energies are denoted with superscript "B", otherwise the energies are BSSE-uncorrected energies.

Hereafter, all of the comments concerning Table 3 take into account the BSSE corrected results at both temperatures. Here, it is important to mention that each part of the overall reaction presented in Figure 3 has its own significance and therefore parallel analysis needs to be made to understand the thermodynamics behind these reactions. The homolytic bond dissociation reactions of isooctane, I-A to I-D, were all endothermic. The least endothermic (the most spontaneous) reaction was I-C, followed by I-B and then I-D and I-A, respectively. Here, it is important to note that the isooctane radical produced in reaction I-C was tertiary, I-B was secondary and I-D and I-A were both primary (Figure 3). The thermodynamic tendencies of the related reactions followed the stabilities of the radicals produced (The radical stability order is known to be $3^{o} > 2^{o} > 1^{o}$). Another point is that the results obtained at 691.15 K were more spontaneous than those at 298.15 K for this stage.

One of the reactions common to all, the homolytic bond dissociation of nitromethane (reaction II), was also endothermic and had a greater tendency at 691.15 K.

The reactions III-A to III-D, combination of the isooctane radicals with nitro radicals to produce nitroisooctanes 1-4, were all exothermic at both temperatures, with a spontaneity order of III-D > III-A > III-B > III-C. From this order, it may obviously be concluded that primary radicals are more reactive than secondary and tertiary radicals when combining with the electron poor nitro radical (Figure 3). The tertiary isooctane radical was the most stable radical in reaction I, and as a result it had a lower tendency to be nitrated. The secondary radical was intermediate in stability and showed more reactive character than the tertiary radical. On the other hand, the primary radicals were the most reactive species to be nitrated, since they were the least stable ones. All of the reactions of step III were found to be more exothermic at 298.15 K.

The other common reaction, the formation of methane from methyl and hydrogen radicals (reaction IV), was also exothermic at both temperatures, but was more favorable at 298.15 K.

In summary, the ΔG values of reactions I-A, II, III-A, and IV gave the ΔG value of the formation of product nitroisooctane-1. Similarly, the sum of the ΔG values of reactions I-B, II, III-B, and IV gave that of the product nitroisooctane-2, and so on (Table 3). The order of the tendencies of the overall reactions for the formation of products at 298.15 K was as nitroisooctane-4 > nitroisooctane-3 > nitroisooctane-1 > nitroisooctane-2, while it was a little different at 691.15 K, as nitroisooctane-4 > nitroisooctane-1 > nitroisooctane-3 > nitroisooctane-2. The formation of the primary nitrated product, nitroisooctane-4, was the most favorable, while that of the secondary one, nitroisooctane-2, was the least favorable at both temperatures. Additionally, the formation reactions at 691.15 K were all endothermic and needed more energy than at 298.15 K. Since higher temperatures may mimic better the real conditions in an engine, the results at 691.15 K are considered to be more feasible than those at 298.15 K. It is also important to note that the BSSE corrections shifted the ΔG values and made them appear more endothermic.

3.3 Ballistic performance

Density (ρ), detonation velocity (D), and detonation pressure (P) are important parameters to evaluate the explosive performance of an energetic material; D and P can be predicted by the Kamlet-Jacobs equations based on the Kistiakowsky-Wilson equation of state [22, 32]. The Kamlet-Jacobs equations are as follows:

$$D = 1.01\ (N\, M_{ave}^{1/2}\, Q^{1/2}\ )^{1/2}\ (1 + 1.30\rho) \quad (2)$$

$$P = 1.558\ \rho^2\, N\, (M_{ave})^{1/2}\, Q^{1/2} \quad (3)$$

Each term in Equations 2 and 3 is defined as: D, detonation velocity (km/s);

P, detonation pressure (GPa); ρ, mass density of explosive (g/cm^3); *N*, moles of gaseous detonation products per gram of explosive (mol/g); M_{ave}, average molecular weight of gaseous products (g/mol); *Q*, chemical energy of detonation (cal/g). Here, the parameters *N*, M_{ave}, and *Q* have been calculated according to the chemical composition of each explosive as listed in the second column of Table 4 [22, 33, 34]. In the table, *M* is the molecular weight of the compound in g/mol; ΔH^o_f is the standard heat of formation of the compound in kJ/mol. The density of each compound is defined as the molecular weight divided by the molar volume as discussed before. Previous studies [35-37] have reported that the standard heat of formation (ΔH^o_f) of an isolated gas phase molecule calculated at the PM3 level could reasonably replace the experimental data in evaluating the detonation velocity (*D*) and detonation pressure (*P*) of the energetic compound, because they are not sensitive to ΔH^o_f but are quite sensitive to the density (ρ).

Table 4. Stoichiometric relations key for calculation of the *N*, M_{ave}, and *Q* parameters of the $C_aH_bO_cN_d$ explosives [22, 33, 34]

Stoichiometric relations			
Parameter	$c \geq 2a + b/2$	$2a + b/2 > c \geq b/2$	$b/2 > c$
N	$(b + 2c + 2d)/4M$	$(b + 2c + 2d)/4M$	$(b + d)/2M$
M_{ave}	$4M/(b + 2c + 2d)$	$(56d + 88c – 8b)/(b + 2c + 2d)$	$(2b + 28d + 32c)/(b + d)$
$Q \times 10^{-3}$	$(28.9b + 94.05a + 0.239\Delta H^o_f)/M$	$[28.9b + 94.05(c/2 – b/4) + 0.239\Delta H^o_f]/M$	$(57.8c + 0.239\Delta H^o_f)/M$

The Kamlet-Jacobs calculations can also be applied to propellants as well as primary and secondary explosives to obtain an overall estimate of their ballistic performances [38]. Accordingly, Table 5 demonstrates the results for nitromethane and nitro-isooctane crystals. In the table, the standard heats of formation were obtained from PM3 single point calculations over DFT UB3LYP/cc-pVDZ optimized structures. Additionally, the average molar volumes were obtained from 100-single point calculations [39] at DFT UB3LYP/cc-pVDZ level of theory. The order of ballistic performance of the nitrated products, from least energetic to most energetic, was: nitroisooctane-4 < nitroisooctane-1 < nitroisooctane-3 < nitroisooctane-2. The corresponding *D* and *P* values varied between 4.43-4.60 km/s and 6.36-7.01 GPa, respectively, and were all lower than the performance values of crystalline nitromethane (*D* = 7.84 km/s and *P* = 24.03 GPa). The difference in performance arose predominantly from the crystal densities, which were calculated as 1.48 g/cm^3 for nitromethane and 1.15-1.18 g/cm^3 for the nitro-

isooctane species. Since nitromethane is normally in the liquid phase and less dense than its crystal phase (1.127 g/cm^3) [5], its ballistic performance also appears to be lower than that of its crystal phase (D = 6.29 km/s, P = 14.1 GPa) [24].

Table 5. Calculated Kamlet-Jacobs detonation performances of nitromethane and the nitro-isooctane products in their crystal phase

	ΔH_f^{o} [a)] [kJ/mol]	M [g/mol]	N [mol/g]	M_{ave} [g/mol]	Q [cal/g]	V^{o} [b)] [cm^3/mol]	ρ [g/cm^3]	D [km/s]	P [GPa]
Nitromethane	−57.90	61.04	0.03686	23.11	1578.87	41.16	1.48 (1.127)[c)]	7.84 (6.29)[c)]	24.03 (14.1)[c)]
Nitroisooctane-1	−190.22	159.23	0.05652	7.00	440.48	137.10	1.16	4.49	6.58
Nitroisooctane-2	−172.36	159.23	0.05652	7.00	467.29	135.33	1.18	4.60	7.01
Nitroisooctane-3	−179.68	159.23	0.05652	7.00	456.299	137.63	1.16	4.53	6.70
Nitroisooctane-4	−200.11	159.23	0.05652	7.00	425.63	138.09	1.15	4.43	6.36

[a)] Standard heats of formation obtained from PM3 single point calculations [35-37] over DFT UB3LYP/cc-pVDZ optimized structures.

[b)] Average molar volumes from 100-single point calculations [39] at DFT UB3LYP/cc-pVDZ theoretical level.

[c)] Data in parentheses are the experimental ρ value [5], and D and P values [24] reported for liquid nitromethane.

The thermodynamic spontaneity order of the reactions at 691.15 K discussed in the previous section showed parallels with the ballistic order of the related products. The spontaneity order of the formation of the nitro-isooctane products was nitroisooctane-4 > nitroisooctane-1 > nitroisooctane-3 > nitroisooctane-2, to which the ballistic (energetic) order was related. The results were self-consistent, *i.e.*, the formation reaction of the least energetic species, nitroisooctane-4, was the most favorable, while the most energetic species, nitroisooctane-2, was the least favorable in terms of the Gibbs free energy of formation. The related values of the other species, nitroisooctane-1 and nitroisooctane-3, were intermediate.

3.4 Specific impulse

The term *specific impulse* can be used to describe and characterize the performance of propellants. It is defined as the thrust divided by the propellant combustion rate. A high explosive can be designated as a monopropellant in which its specific impulse depends upon chemical and structural factors. A simple method can be used to estimate the specific impulse of mostly ideal and less ideal

composition explosives from the detonation velocity of the explosive, which can be designated as a monopropellant, and its crystal density. The simple empirical equation has the form [23, 24]:

$$I_{SP} = (D - 1.98) / (1.453\rho) \quad (4)$$

where D is the detonation velocity in km/s, ρ is the crystal density in g/cm^3, and I_{SP} is the specific impulse in Ns/g. The calculated I_{SP} values for crystalline nitromethane and the nitroisooctanes 1-4 are listed in Table 6. The values for the nitro-isooctanes varied between 1.47-1.53 Ns/g. The I_{SP} order was nitroisooctane-2 > nitroisooctane-3 > nitroisooctane-1 > nitroisooctane-4, which is also consistent with the ballistic (energetic) order. For instance, the most energetic species, nitroisooctane-2, had the highest specific impulse, while the least energetic one, nitroisooctane-4, had the lowest. The values of the other species, nitroisooctane-1 and nitroisooctane-3, were intermediate. All of the nitro-isooctane species had lower specific impulses than solid nitromethane (2.73 Ns/g) due to their lower crystal densities and detonation velocities. Similarly, having a lower detonation velocity and density made liquid nitromethane weaker than solid nitromethane (I_{SP} = 2.63 Ns/g) (Table 6).

Table 6. Calculated specific impulse (I_{SP}) values for crystalline nitromethane and the nitroisooctanes 1-4

	D [km/s]	ρ [g/cm^3]	I_{SP}[a)] [Ns/g]
Nitromethane	7.84	1.48	2.73
	6.29[b)]	1.127[b)]	2.63
Nitroisooctane-1	4.49	1.16	1.49
Nitroisooctane-2	4.60	1.18	1.53
Nitroisooctane-3	4.53	1.16	1.51
Nitroisooctane-4	4.43	1.15	1.47

[a)] Calculated I_{SP} values using Equation 4. D and ρ are all calculated values.
[b)] Experimental D [24] and ρ [5] values for liquid nitromethane.

3.5 Heat of combustion and deflagration temperature

The heats of combustion of nitromethane and of the nitroisooctanes 1-4 were calculated according to the empirical formula based on $C_aH_bN_cO_d$ type explosives reported in the study by Keshavarz *et al.* [40]. The calculated value for nitromethane was −719.1 kJ/mol; the experimental value was determined as −709.6 kJ/mol in the study by Lebedeva and Ryadenko [41]. Since all of the nitroisooctanes 1-4 had

the same molecular formula and were all the constitutional isomers of each other, they had the same calculated value of the heat of combustion (−5183.0 kJ/mol). This was a reasonable result since the nitro-isooctanes were all larger molecules than nitromethane and had the potential to release more energy.

The deflagration temperatures were calculated according to the empirical formula derived by Keshavarz *et al*., based on carbon and oxygen numbers and some other structural parameters of the energetic materials [42]. By similar reasoning, all of the nitroisooctanes 1-4 had the same deflagration temperature of 569 K, since they had the same numbers of carbon and oxygen atoms. Nitromethane had a lower deflagration temperature of 477 K. Since nitromethane propellant has a more energetic character than the nitroisooctanes 1-4 fuels, a relatively lower temperature is required to deflagrate it.

4 Conclusions

The conclusions of this study can be listed with some major outcomes:

a) The cc-pVDZ basis set of DFT UB3LYP theoretical level was chosen as an ideal basis set for the calculations since it gave values closest to reported experimental values for both the crystal density and the structural parameters of solid nitromethane propellant.
b) The possible radical nitrations of isooctane with nitromethane at high temperature (691.15 K, which is the auto-ignition temperature of both components) were all found to be endothermic.
c) The most favorable nitration reaction gave nitroisooctane-4 (product of nitration at a primary carbon) while the least favorable one gave nitroisooctane-2 (product of nitration at a secondary carbon). The products of nitration at the other primary and tertiary positions, nitroisooctane 1 and 3, were intermediate in terms of spontaneity.
d) The thermodynamic tendencies of the reactions discussed in "c" parallelled the products' ballistic performances. The product of the least favourable nitration reaction, nitroisooctane-2, was the strongest, while the product of the most favourable nitration reaction, nitroisooctane-4, was the weakest in terms of their ballistic performances, such as detonation velocity, detonation pressure and specific impulse. The ballistic performances of the other two nitrated species, nitroisooctane 1 and 3, were intermediate, as in the case of "c".
e) The heats of combustion of the nitroisooctanes 1-4 (−5183.0 kJ/mol for all) were found to be higher than that of nitromethane (−709.6 kJ/mol). This

was an expected result since the larger isooctanes had more potential to release energy.

f) The deflagration temperatures of nitromethane and the nitroisooctanes 1-4 were calculated as 477 and 569 K, respectively. Nitromethane is a more energetic material and acts as a propellant while the nitroisooctanes 1-4 are less energetic materials and therefore have fuel characteristics. This factor makes fuels thermally more stable and causes them to deflagrate at relatively higher temperatures.

Acknowledgement

I would like to thank to Bulent Ecevit University Scientific Research Projects Coordination Office for financial support (Project No. BAP-2016-73338635-02).

References

[1] Sax, N. I.; Lewis, Sr., R. J. *Hawley's Condensed Chemical Dictionary.* 11th ed., Van Nostrand Reinhold Co., New York **1987**, p. 658; ISBN 9780442280970.

[2] Budavari, S. *The Merck Index: An Encyclopedia of Chemicals, Drugs, and Biologicals*. 11th ed., Merck and Co., Inc., Rahway, NJ **1989**, p. 817; ISBN 9780911910285.

[3] *Fire Protection Guide to Hazardous Materials.* 12th ed., National Fire Protection Association, Quincy, MA **1997**, pp. 325-362; ISBN 9780877654278.

[4] Auzmendi-Murua, I.; Bozzelli, J. W. Thermochemistry, Reaction Paths, and Kinetics on the Secondary Isooctane Radical Reaction with $^3O_2$. *Int. J. Chem. Kinet.* **2014**, *46*(2): 71-103.

[5] Warren, W. C. *Experimental Techniques for the Study of Liquid Monopropellant Combustion*. MSc Thesis, Texas A&M University, **2012**.

[6] Bush, K. C.; Germane, G. J.; Hess, G. L. *Improved Utilization of Nitromethane as an Internal Combustion Engine Fuel*. SAE Technical Paper 852130, **1985**.

[7] Zhang, Y. X.; Bauer, S. H. The Gas-Phase Pyrolysis of 2,2-Dinitropropane: Shock-Tube Kinetics. *J. Phys. Chem. A* **2000**, *104*(6): 1217-1225.

[8] Steinberger, R. L.; Santavicca, D. A.; Bruno, B. A.; Daly, D. T. *A Comparison of the Effects of Additives on Spark Ignited Combustion in a Laminar Flow System and in an Engine under Cold Start Conditions*. SAE Technical Paper 2002-01-2834, **2002**.

[9] Ma, H.; Kar, K.; Stone, R.; Raine, R.; Thorwarth, H. Analysis of Combustion in a Small Homogeneous Charge Compression Assisted Ignition Engine. *Int. J. Engine Res.* **2006**, *7*(3): 237-253.

[10] Cracknell, R. F.; Andrae, J. C. G.; McAllister, L. J.; Norton, M.; Walmsley, H. L. The Chemical Origin of Octane Sensitivity in Gasoline Fuels Containing Nitroalkanes.

Combust. Flame **2009**, *156*(5): 1046-1052.
[11] Stewart, J. J. P. Optimization of Parameters for Semiempirical Methods. I Method. *J. Comput. Chem.* **1989**, *10*(2): 209-220.
[12] Young, D. C. *Computational Chemistry*. 1st ed., Wiley, New York **2001**, pp. 19-21; ISBN 0471333689.
[13] Kohn, W.; Sham, L. J. Self-consistent Equations Including Exchange and Correlation Effects. *Phys. Rev.* **1965**, *140*(4A): A1133-A1138.
[14] Becke, A. D. Density-functional Exchange-energy Approximation with Correct Asymptotic Behavior. *Phys. Rev. A* **1988**, *38*(6): 3098-3100.
[15] Vosko, S. H.; Wilk, L.; Nusair, M. Accurate Spin-dependent Electron Liquid Correlation Energies for Local Spin Density Calculations: A Critical Analysis. *Can. J. Phys.* **1980**, *58*(8): 1200-1211.
[16] Lee, C.; Yang, W.; Parr, R. G. Development of the Colle-salvetti Correlation-energy Formula into a Functional of the Electron Density. *Phys. Rev. B* **1988**, *37*(2): 785-789.
[17] *Fire Protection Guide to Hazardous Materials.* 14th ed., National Fire Protection Association, Quincy, MA **2010**, pp. 325-392; ISBN 9781616650414.
[18] Ebrahimi, A.; Karimi, P.; Akher, F. B.; Behazin, R.; Mostafavi, N. Investigation of the π-π Stacking Interactions without Direct Electrostatic Effects of Substituents: the Aromatic||Aromatic and Aromatic||Anti-aromatic Complexes. *Mol. Phys.* **2014**, *112*(7): 1047-1056.
[19] Mudedla, S. K.; Balamurugan, K.; Subramanian, V. Computational Study on the Interaction of Modified Nucleobases with Graphene and Doped Graphenes. *J. Phys. Chem. C* **2014**, *118*(29): 16165-16174.
[20] Boys, S. F.; Bernardi, F. The Calculation of Small Molecular Interactions by the Differences of Separate Total Energies. Some Procedures with Reduced Errors. *Mol. Phys.* **1970**, *19*(4): 553-566.
[21] Mottishaw, J. D.; Sun, H. Effects of Aromatic Trifluoromethylation, Fluorination, and Methylation on Intermolecular π-π Interactions. *J. Phys. Chem. A* **2013**, *117*(33): 7970-7979.
[22] Kamlet, M. J.; Jacobs, S. J. Chemistry of Detonations. I: A Simple Method for Calculating Detonation Properties of C-H-N-O Explosives. *J. Chem. Phys.* **1968**, *48*(1): 23-35.
[23] Keshavarz, M. H. Prediction Method for Specific Impulse Used as Performance Quantity for Explosives. *Propellants Explos. Pyrotech.* **2008**, *33*(5): 360-364.
[24] Keshavarz, M. H.; Motamedoshariati, H.; Moghayadnia, R.; Nazari, H. R.; Azarniamehraban, J. A New Computer Code to Evaluate Detonation Performance of High Explosives and Their Thermochemical Properties, Part I. *J. Hazard. Mater.* **2009**, *172*(2-3): 1218-1228.
[25] Frisch, M. J.; Trucks, G. W.; Schlegel, H. B.; Scuseria, G. E.; Robb, M. A.; Cheeseman, J. R.; Scalmani, G.; Barone, V.; Mennucci, B.; Petersson, G. A.; Nakatsuji, H.; Caricato, M.; Li, X.; Hratchian, H. P.; Izmaylov, A. F.; Bloino, J.; Zheng, G.; Sonnenberg, J. L.; Hada, M.; Ehara, M.; Toyota, K.; Fukuda, R.;

Hasegawa, J.; Ishida, M.; Nakajima, T.; Honda, Y.; Kitao, O.; Nakai, H.; Vreven, T.; Montgomery Jr., J. A.; Peralta, J. E.; Ogliaro, F.; Bearpark, M.; Heyd, J. J.; Brothers, E.; Kudin, K. N.; Staroverov, V. N.; Kobayashi, R.; Normand, J.; Raghavachari, K.; Rendell, A.; Burant, J. C.; Iyengar, S. S.; Tomasi, J.; Cossi, M.; Rega, N.; Millam, J. M.; Klene, M.; Knox, J. E.; Cross, J. B.; Bakken, V.; Adamo, C.; Jaramillo, J.; Gomperts, R.; Stratmann, R. E.; Yazyev, O.; Austin, A. J.; Cammi, R.; Pomelli, C.; Ochterski, J. W.; Martin, R. L.; Morokuma, K.; Zakrzewski, V. G.; Voth, G. A.; Salvador, P.; Dannenberg, J. J.; Dapprich, S.; Daniels, A. D.; Farkas, O.; Foresman, J. B.; Ortiz, J. V.; Cioslowski, J.; Fox, D. J. *Gaussian 09*, *Revision E.01*. Gaussian, Inc., Wallingford CT **2013**.

[26] Appalakondaiah, S.; Vaitheeswaran, G.; Lebègue, S. A DFT Study on Structural, Vibrational Properties, and Quasiparticle Band Structure of Solid Nitromethane. *J. Chem. Phys*. **2013**, *138*(18): (184705-1)-(184705-12).

[27] Trevino, S. F.; Prince, E.; Hubbard, C. R. Refinement of the Structure of Solid Nitromethane. *J. Chem. Phys.* **1980**, *73*(6): 2996-3000.

[28] Conroy, M. W. *Density Functional Theory Studies of Energetic Materials*. PhD Dissertation, University of South Florida, **2009**.

[29] Bader, R. F. W.; Carroll, M. T.; Cheeseman, J. R.; Chang, C. Properties of Atoms in Molecules: Atomic Volumes. *J. Am. Chem. Soc.* **1987**, *109*(26): 7968-7979.

[30] Liu, H.; Zhao, J.; Wei, D.; Gong, Z. Structural and Vibrational Properties of Solid Nitromethane under High Pressure by Density Functional Theory. *J. Chem. Phys.* **2006**, *124*(12): (124501-1)-(124501-10).

[31] Baik, J.; Kim, J.; Majumdar, D.; Kim, K. S. Structures, Energetics, and Spectra of Fluoride-Water Clusters $F^-(H_2O)_n$, n = 1-6: *ab initio* Study. *J. Chem. Phys*. **1999**, *110*(18): 9116-9127.

[32] Akhavan, J. *The Chemistry of Explosives*. 2nd ed., The Royal Society of Chemistry, UK **2004**, pp. 78-80; ISBN 0854046402.

[33] Wang, G.; Gong, X.; Liu, Y.; Xiao, H. A Theoretical Investigation on the Structures, Densities, Detonation Properties, and Pyrolysis Mechanism of the Nitro Derivatives of Phenols. *Int. J. Quantum Chem.* **2010**, *110*(9): 1691-1701.

[34] Liu, Y.; Gong, X.; Wang, L.; Wang, G.; Xiao, H. Substituent Effects on the Properties Related to Detonation Performance and Sensitivity for 2,2',4,4',6,6'-Hexanitroazobenzene Derivatives. *J. Phys. Chem. A* **2011**, *115*(9): 1754-1762.

[35] Akutsu, Y.; Tahara, S.-Y.; Tamura, M.; Yoshida, T. Calculations of Heats of Formation for Nitro Compounds by Semi-Empirical MO Methods and Molecular Mechanics. *J. Energ. Mater.* **1991**, *9*(3): 161-171.

[36] Dorsett, H.; White, A. *Overview of Molecular Modelling and ab initio Molecular Orbital Methods Suitable for Use with Energetic Materials*. Weapons Systems Division, Aeronautical and Maritime Research Laboratory, Australia, DSTO-GD-0253, **2000**.

[37] Sikder, A. K.; Maddala, G.; Agrawal, J. P.; Singh, H. Important Aspects of Behaviour of Organic Energetic Compounds: A Review. *J. Hazard. Mater.* **2001**,

84(1): 1-26.
[38] Zhao, J.; Jin, B.; Peng, R.; Liu, Q.; Tan, B.; Chu, S. Synthesis and Characterization of a New Energetic Salt Based on Dinitramide. *Z. Anorg. Allg. Chem.* **2015**, *641*(15): 2630-2636.
[39] Qiu, L.; Xiao, H.; Gong, X.; Ju, X.; Zhu, W. Theoretical Studies on the Structures, Thermodynamic Properties, Detonation Properties and Pyrolysis Mechanisms of Spiro Nitramines. *J. Phys. Chem. A* **2006**, *110*(10): 3797-3807.
[40] Keshavarz, M. H.; Saatluo, B. E.; Hassanzadeh, A. A New Method for Predicting the Heats of Combustion of Polynitro Arene, Polynitro Heteroarene, Acyclic and Cyclic Nitramine, Nitrate Ester and Nitroaliphatic Compounds. *J. Hazard. Mater.* **2011**, *185*(2-3): 1086-1106.
[41] Lebedeva, N. D.; Ryadenko, V. L. R. Enthalpies of Formation of Nitroalkanes. *Russ. J. Phys. Chem. (Engl. Transl.)* **1973**, *47*: 1382.
[42] Keshavarz, M. H.; Moradi, S.; Saatluo, B. E.; Rahimi, H.; Madram, A. R. A Simple Accurate Model for Prediction of Deflagration Temperature of Energetic Compounds. *J. Therm. Anal. Calorim.* **2013**, *112*(3): 1453-1463.